Author Manuscript

Author Manuscript

Author Manuscript

Author Manuscript

HHS Public Access

Author manuscript

Ann Thorac Surg. Author manuscript; available in PMC 2017 September 01.

Published in final edited form as:

Ann Thorac Surg. 2016 September ; 102(3): 780–786. doi:10.1016/j.athoracsur.2016.02.082.

Design of a Coupled Thermoresponsive Hydrogel and Robotic System for Postinfarct Biomaterial Injection Therapy

Yang Zhu, MS[#], **Nathan A. Wood, PhD**[#], **Kevin Fok, MS**, **Tomo Yoshizumi, MD**, **Daewoo Park, PhD**, **Hongbin Jiang, MD**, **David S. Schwartzman, MD**, **Marco A. Zenati, MD**, **Takafumi Uchibori, MD**, **William R. Wagner, PhD**[#], and **Cameron N. Riviere, PhD**[#]

McGowan Institute for Regenerative Medicine and Department of Bioengineering, University of Pittsburgh, Pittsburgh; The Robotics Institute, Carnegie Mellon University, Pittsburgh; Heart and Vascular Institute and Center for Ultrasound Molecular Imaging and Therapeutics, University of Pittsburgh, Pittsburgh; Department of Surgery, Harvard University, Boston, Massachusetts; and Departments of Surgery and Chemical Engineering, University of Pittsburgh, Pittsburgh, Pennsylvania

[#] These authors contributed equally to this work.

Abstract

Background—In preclinical testing, ventricular wall injection of hydrogels has been shown to be effective in modulating ventricular remodeling and preserving cardiac function. For some approaches, early-stage clinical trials are under way. The hydrogel delivery method varies, with minimally invasive approaches being preferred. Endocardial injections carry a risk of hydrogel regurgitation into the circulation, and precise injection patterning is a challenge. An epicardial approach with a thermally gelling hydrogel through the subxiphoid pathway overcomes these disadvantages.

Methods—A relatively stiff, thermally responsive, injectable hydrogel based on N-isopropylacrylamide and N-vinylpyrrolidone (VP gel) was synthesized and characterized. VP gel thermal behavior was tuned to couple with a transepicardial injection robot, incorporating a cooling feature to achieve injectability. Ventricular wall injections of the optimized VP gel have been performed ex vivo and on beating porcine hearts.

Results—Thermal transition temperature, viscosity, and gelling time for the VP gel were manipulated by altering N-vinylpyrrolidone content. The target parameters for cooling in the robotic system were chosen by thermal modeling to support smooth, repeated injections on an ex vivo heart. Injections at predefined locations and depth were confirmed in an infarcted porcine model.

Conclusions—A coupled thermoresponsive hydrogel and robotic injection system incorporating a temperature-controlled injectate line was capable of targeted injections and amenable to use with a subxiphoid transepicardial approach for hydrogel injection after myocardial infarction. The

Address correspondence to Dr Wagner, 450 Technology Dr, Ste 300, Pittsburgh, PA 15219; wagnerwr@upmc.edu.

The Appendices and Videos can be viewed on the online version of this article [http://dx.doi.org/10.1016/j.athoracsur.2016.02.082] on http://www.annalsthoracicsurgery.org.

Author Manuscript Author Manuscript Author Manuscript Author Manuscript

confirmation of precise location and depth injections would facilitate a patient-specific planning strategy to optimize injection patterning to maximize the mechanical benefits of hydrogel placement.

Pathologic remodeling of the ventricular wall after myocardial infarction (MI) can ultimately lead to endstage heart failure and death. The loss of myocardium after MI results in an abrupt increase in loading conditions, causing a unique pattern of remodeling involving the feedback loop of higher wall stress, left ventricle (LV) dilatation, and a thinning ventricular wall [1]. The injection of hydrogels into and around the infarcted myocardium has been shown to be effective in preventing ventricular remodeling and maintaining cardiac function putatively by providing mechanical support [2–5]. Recently, clinical trials have been launched in an effort to translate intramyocardial hydrogel injection therapy to the bedside [6–8]. One of the advantages of hydrogel injection therapy is its potential to be delivered in a minimally invasive fashion; for instance, Seif-Naraghi and colleagues [9] successfully injected extracellular matrix–derived hydrogel by a percutaneous, transendocardial intervention and Leor and colleagues [10] delivered alginate by intracoronary infusion, both in pig models. Both techniques approach the injection sites by catheter originating through a femoral artery access site. No remote infarction or embolization was reported in either pig model; however, there are theoretic safety concerns associated with the potential for hydrogel leakage into the circulatory system.

Here we report an alternative option for minimally invasive delivery of a hydrogel to the LV wall without entrance into the circulatory system and with reduction of concerns about hydrogel regurgitation into the circulating blood volume. An injection strategy facilitated by the coordinated design of a thermoresponsive hydrogel and a robotic injection device using local temperature control is described. A biodegradable, thermoresponsive hydrogel was synthesized, and its thermal behavior was modulated to facilitate robotic injection. A previously reported robotic system, HeartLander [11], was modified to incorporate a fluid cooling system and redesign of the injection pathway to provide the capacity of delivering thermally sensitive materials. Injections were attempted in a pig model through a subxiphoid transepicardial approach with a predefined injection pattern and depth to show the precision and efficacy of the strategy.

To effectively deliver the thermoresponsive hydrogel, three efforts were coordinated, as shown in Figure 1. The first component was the design of the injectable hydrogel, thermoresponsive poly(NIPAAm-co-VP-co-MAPLA) (NIPAAm: N-isopropylacrylamide, VP: N-vinylpyrrolidone, MAPLA: methacrylate-polylactide), which gels from a low-viscosity solution as the temperature increases to 37°C. The second component was the modification of the robotic injection system to effectively cool the hydrogel solution, crawl on a beating heart, and make injections in a controlled manner. The third component was the real-time tracking system that maps the three-dimensional (3D) structure of the working field and localizes the robotic injection system to guide the crawler to the desired positions while avoiding major blood vessels. During the procedure, small subxiphoid and pericardial incisions allow access of the crawler head region to the LV epicardial wall, and the hydrogel is injected extracorporeally. The polymer solution is kept cool by a coaxial cooling fluid

Author Manuscript Author Manuscript Author Manuscript Author Manuscript

pathway up to the point of injection, where the injected material undergoes phase transformation within the targeted region of the LV wall.

Material and Methods

Materials

All chemicals were purchased from Sigma-Aldrich. The N-isopropylacrylamide (NIPAAm) was purified by recrystallization from hexane and vacuum-dried. The N-vinylpyrrolidone (VP), lactide, benzoyl peroxide (BPO), sodium methoxide ($NaOCH_3$), methacryloyl chloride, methacrylic acid, and other solvents were used as received.

Synthesis of poly(NIPAAm-co-VP-co-MAPLA)

The MAPLA was synthesized as previously described [12]. Poly(NIPAAm-co-VP-co-MAPLA) copolymers were synthesized from NIPAAm, VP, and MAPLA by free radical polymerization. The feed ratios of NIPAAm, VP, and MAPLA were 80/j/(20-j), where j = 10, 15, 17.5, 20, and the corresponding product polymers were named as VPj (eg, VP10). (See Appendix, supporting information, for details of the polymer synthesis.) For photoacoustic (PA) imaging described below, 48 mg/mL indocyanine green (ICG) was dissolved in VP15 hydrogel before injection.

Characterization

^1H nuclear magnetic resonance (NMR) spectra of poly(NIPAAm-co-VP-co-MAPLA) copolymers were recorded with a 600-MHz Bruker spectrometer using CD_3Cl as solvent. Rheology measurements were performed as previously described [12].

To measure the transition time of hydrogels in 37°C air, 150 mL of each type of hydrogel was added to a precooled (0°C) 96-well plate and placed in a plate reader that was prewarmed to and set at 37°C. Absorbance at 490 nm was recorded for 15 minutes.

VP10 and VP15 degradation was quantified by mass loss measurements. Hydrogels with known initial dry masses (w60 mg) were immersed into 6 mL of PBS (replaced weekly to maintain a constant pH value of 7) at 37°C. At predefined time points over a 10-week period, the hydrogels (n = 3 each) were lyophilized, and the relative mass loss was recorded.

Injection studies in rats were performed as previously described except that the end point was set at 28 days after injection [12].

Robotic Injection System Modified With Cooling Line

Modifications to an existing HeartLander injection robot [13] were made to accomodate the dual-lumen cooled injection system, including moving the injection channel to the rear foot and widening the robot from 8 to 9.85 mm. These modifications minimized the effect of increased tether stiffness on robot mobility. The cooled injection system consisted of inner and outer polytetrafluoroethylene (PTFE) tubes of 23 and 17 gauge, respectively. A diagram of the modified robot and injection system is shown in Figure 1.

Author Manuscript Author Manuscript Author Manuscript Author Manuscript

Simulation Model

A computational model of the parallel-flow heat exchanger model was developed with the use of COM-SOL Multiphysics software to determine (1) the required cooling fiuid flow rate and (2) the size of the outer PTFE tube of the injection system. The implemented model was intended to provide estimates for the worst-case operating scenario of the cooling system, namely, when the device was deployed on the heart and the injection catheter was filled with solidified, body-temperature hydrogel. (More details of the simulation can be found in the Appendix, supporting information).

Water Bath Study

By use of the results obtained from the simulation environment, a peristaltic pump (Stenner 85MHP17, Stenner Pump Company, Jacksonville, FL) was identified that could provide sufficient flow to cool the hydrogel. A length of 0.30-m of the hydrogel-filled injection system was submerged in a 0.30-m x 0.14-m x 0.03-m container filled with water at 36.5 to 37.5°C. The distal end of the injection system protruded from the container and emptied the cooling fluid outside of the system. A thermocouple with attached microprobe was inserted to measure the hydrogel temperature at 0.05-m intervals along the tube. Water at 0°C to 3°C was used as the cooling fluid and pumped at a rate of 44 mL/min. The measured temperature of the cooling fluid at the inlet to the injection system was 12.5°C.

Hydrogel was loaded into the injection system and allowed to reach 37°C. Once the hydrogel had reached the temperature of the water bath, the pump was started, and temperature measurements of the hydrogel were taken at intervals of 1 second for approximately 3 minutes to ensure steady state. This procedure was performed three times for each temperature measurement, and the averages were used for comparison to the heat transfer model.

Beating Heart Injections in Porcine Model

A demonstration of the modified injection system design was then performed in a porcine model in vivo in a protocol that followed the National Institutes of Health guidelines for animal care and that was approved by the University of Pittsburgh's Institutional Animal Care and Use Committee. Testing with the VP15 hydrogel, PA imaging, and depth control were carried out on the first animal, and patterned injections were performed on the second animal.

A preoperative static 3D computed tomography (CT) image dataset was collected to provide image guidance during the procedure and to plan the desired injection pattern on the epicardial surface. Surface models of the pericardium, endocardium, cardiac vasculature, rib cage, and fiducial markers on the chest wall were constructed from the 3D image set. A 15-mm square injection pattern was selected on the anterior surface of the left ventricle between the anterior interventricular artery and the diagonal artery. Saline cooling fluid and VP15 hydrogel were precooled before the procedure.

During the procedure, the heart was allowed to beat naturally, and artificial ventilation was used to regulate respiration at a rate of 12 breaths/min. Access to the apex of the heart was

Author Manuscript Author Manuscript Author Manuscript Author Manuscript

achieved through a subxiphoid skin incision and a second small incision in the pericardium. Injecting head sections of the robotic device were placed onto the epicardium, under the pericardium, through these incisions. Once placed on the heart, the device was manually controlled by virtual image guidance in which a virtual view of the robot and anatomy were displayed to the surgeon on the control computer.

Before the first target was reached, both the inner and outer lumens of the injection line were kept empty to limit the volume of water expelled into the pericardial space. Upon acquisition of the first target, the cooling fiuid was first pumped through the system at a flow rate of 44 mL/min. Next, hydrogel was introduced to completely fill the inner lumen. The needle tip was then advanced into the myocardium, and 0.5 mL of cooled hydrogel was injected into the LV wall. The needle was then retracted. With the injection line filled with hydrogel and the cooling fluid continuing to flow, the robot was driven to the second injection site, where another injection was performed. After the second site was injected, the robot was removed from the animal and visually inspected to ensure that no solidification of the hydrogel had occurred in the inner lumen. Saline was pushed through the injection line to ensure that the line was free of occlusion. After inspection, the robotic device was once again placed on the heart, and the procedure was repeated for the third and fourth injection targets.

Upon completion of the injections, the animal was euthanized, and the heart was excised and placed in a warm saline bath. Neither identiflable needle tracks nor backflow of the hydrogel was visually inspected. Photo-acoustic imaging was performed to localize the hydrogel material in the excised heart. Quantitative comparison of the planned and actual injection locations was done to determine the positioning accuracy of the modified injection device. The locations of the injection sites in the PA image were calculated by first segmenting the fore-ground pixels using k-means clustering, then computing the intensity-weighted centroid of each cluster. To compare the actual injection locations with the planned injection locations, the rigid registration between the imaged points and the planned points was solved with the use of least squares. A scaling factor was also included to account for the post-mortem shrinkage of the heart [14].

Results

Thermoresponsive poly(NIPAAm-co-VP-co-MAPLA) with varied composition was synthesized by radical polymerization, and its structure was confirmed with NMR (Figs 2a and 2b). In the polymer design, NIPAAm provides thermal responsiveness, and increasing VP content tunes the hydrophilicity for lower viscosity, higher transition temperatures, and longer transition times. MAPLA, incorporating hydrolytically labile PLA segments, provides an “insoluble to soluble” shift to the whole polymer at body temperature as these hydro-phobic segments are cleaved. To ensure smooth injection without solidifying the hydrogel in the catheter, a hydrogel with a higher transition temperature is more attractive. As shown in Figure 2c, the transition temperature increases as the VP feed ratio used in the polymer synthesis increases, from 19°C (VP10) to an undiscernible transition (VP20, turbidity increase at elevated temperature observed), consistent with increased hydrophilicity. In addition, the viscosity of the hydrogel in the solution state decreased with the increased VP content, which also favored easier hydrogel delivery. Whereas the

Author Manuscript Author Manuscript Author Manuscript Author Manuscript

synthesized hydrogels underwent thermal transition immediately upon contact with 37°C saline, in 37°C air the transition was slowed for the more hydrophilic compositions (Fig 2d). This property helped the hydrogel to stay in solution form along the injection pathway from outside to inside the body. Mechanical characterization of the hydrogels at 37°C demonstrated that hydrogels VP17.5 and VP20 were too weak to be handled in testing and were not assessed further, whereas VP10 and VP15 were further evaluated (VP10: 240 ± 49 kPa; VP15: 21 ± 4 kPa). Both hydrogels completely dissolved in 37°C saline after 7 to 10 weeks of incubation, with more hydrophilic VP15 showing faster solubilization, as shown in Figure 2e. In biocompatibility testing, both hydrogels induced a typical foreign body response in vivo when injected into the rat hindlimb muscle for 28 days, without signs of local or systemic toxicity. Histologic evaluation demonstrated local macrophage involvement at the injection site, with the number of macrophages (CD68 positive staining) being greater for the VP10 hydrogel. The injection site also demonstrated a residual region of hydrogel for VP10, whereas for the faster solubilizing VP15 no distinct polymer region was found (Fig 2f, Appendix Figure S1).

In the new version of the injection system, a cooling sheath was added to provide cooling fluid running parallel to the hydrogel solution (Fig 3a). A simulation of the temperature distribution of the hydrogel was found to be insensitive to changes in the thermal conductivity (0.2 to 40 W m^{-1} K^{-1}) of the hydrogel. Simulation results with varied cooling fluid flow rates and outer tube diameters showed that the greatest influencers on the hydrogel temperature distribution were the cooling fluid inlet temperature and flow rate. Changing the tube diameter from 15 to 17 gauge had little effect on the hydrogel temperature profile, leading to the choice of 17-gauge outer tubing to minimize tether stiffness, and a cooling fluid flow rate of 44 mL/min to keep the hydrogel well below 27°C (Fig 3b). The injection system with the cooling sheath incorporated was loaded with hydrogel and initially tested in a 37°C water bath for its cooling effect. Time traces of the temperature of the hydrogel at various points along the length of the cooling system are shown in Figure 3c. The cooling system lowered the temperature of the hydrogel to a minimum in approximately 10 seconds where the temperatures increased slightly and settled to steady-state values. The steady-state values along the entire length (0.3 m) of the injection system were well below the transition temperature of VP15 (Fig 3d). Within the first 0.2 m, the steady-temperature was near or below the transition temperature of VP10. Inasmuch as the distance from the subxiphoid incision to the epicardial injection injection sites would be less than 1.3 m, the hydrogel would be expected to remain in the liquid state.

To evaluate the coordination between hydrogel and the cooling system, the catheter was preloaded with hydrogel and submerged in a 37°C water bath to reach an isothermal state, followed by active cooling. Both VP10 and VP15 gelled and occluded the catheter at 37°C, and in both cases the hydrogels were dissolved as a result of heat transfer with the cooling fluid, allowing reoccurence of smooth injections. The unblocking process took approximately 10 seconds for VP15 and approximately 45 seconds for VP10 (Video S1,2), remarkably consistent with the measured time required for the cooling system to bring the hydrogel temperature down to near transition temperature (Fig 3c). This feature of lower potential for catheter occlusion and faster occlusion recovery again favored VP15 in terms of both safety and efficiency of the procedure, in addition to the reduced viscosity (easier

Author Manuscript Author Manuscript Author Manuscript Author Manuscript

injection) and slower phase transition of VP15 compared with VP10 (less occlusion in the needle). When the aforementioned aspects were taken into consideration, VP15 was chosen for further ex vivo and in vivo experiments. In an ex vivo injection test using an excised porcine heart at 37°C, the injection device successfully crawled to two distant injection sites and performed one shallow injection at 3.5 mm deep and one deeper injection at 6.8 mm deep, as shown in Video S3,4 and Appendix Figure S2. The injection depth was controlled by the distance the needle was pushed out of the catheter, as demonstrated in Video S5. The hydrogel temperature was maintained below the hydrogel transition temperature, and no gelation was observed in fluid pathway. It took approximately 10 seconds to complete the injection of 0.3 mL VP15 hydrogel. Visual inspection of the site by dissection 5 minutes after the injection showed ellipsoid hydrogel deposits with long axes orienting along the circumferential direction. The shallow deposit was 10.8 mm long and 3.1 mm wide, whereas the deeper deposit was 8.2 mm long and 2.7 mm wide (Appendix Fig S2).

Hydrogel injections in healthy beating porcine hearts were performed to validate the concept of the subxiphoid transepicardial injection strategy and to demonstrate the potential to perform injections in a predefined pattern as might be planned in a patientspecific manner for an ischemic area after an MI. During the procedure, the crawler was manually controlled to approach the first target site without loading of the hydrogel until the time of injection. Hydrogel was not retrieved from the catheter but remained in the injection pathway for the subsequent injections. With the cooling system functioning, smooth injections were achieved without observing hydrogel clotting of the catheter. No hydrogel leakage was observed on the epicardial surface of excised heart, as a result of rapid gelation of hydrogel upon contact with warm myocardium. No arrhythmias or other severe adverse events were observed. As shown in Figure 4a, four distinct injection sites in a square pattern can be identified near the cardiac apex under PA imaging. The observed injection sites were placed in the preoperative 3D virtual view of the animal to compare with the preplanned injection sites as marked by black crosses (Fig 4b). The overlaid PA image shows that the injection pattern accurately matches the desired pattern with a mean error of 1.4 ± 0.5 mm. Owing to the artifactual reduction in size of the heart upon explantation, the measured square was smaller than both that planned and that recorded during the procedure. The calculated scaling factor was determined to be 1.87, meaning that the post-mortem reduction in excised heart size was approximately 47%, which is consistent with the observations of Hartshorne and Reynolds [14]. In addition to the accuracy in injection localization, reliability in depth control was also achieved, as indicated by the ability to image the four injection sites in the same plane with PA imaging. Rapid hydrogel gelation limited the occurence of diffusion in the healthy myocardium. Consistently, the injected hydrogels could be found approximately 7 mm underneath the epicardial surface in both animals undergoing the surgical procedures, as shown in Figure 4c. The morphologic integration of the hydrogel with the myocardium was similar to that observed in the ex vivo test. Deeper injections about 15 mm underneath the epicardial surface could also be achieved by inserting the needle closer to the endocardial surface in such a manner that the dyed hydrogel could be directly visualized (Fig 4d). Given the angle of the injection system, 0 to 12.5 mm of the metallic needle was exposed to 37°C tissue instead of being protected by cooling fluid as in the catheter. Despite this uncooled

Author Manuscript Author Manuscript Author Manuscript Author Manuscript

region in the needle, it was found that multiple injections of the VP15 hydrogel could be accomplished without occlusion, as in the ex vivo test.

Comment

The coordinated design of a thermoresponsive hydrogel and a robotic injection device using local temperature control has been accomplished in such a manner that the hydrogel was compatible with cardiac wall injection. Further, this hydrogel could be delivered in a targeted fashion into a beating heart in a large animal model. Such targeted delivery would be compatible with a patient-specific planning strategy to optimize the mechanical benefits of the hydrogel bulking effect [15, 16]. Previous experimentation has shown the ability of HeartLander to reach the posterior surface of the heart and for this device to map electric activity, although the latter functionality was not present on the device used for these studies [11, 17]. The efficacy of the hydrogel therapy has not been the subject of this study, and longterm large animal studies in animals with MI would be necessary. However, similar synthetic hydrogels have shown benefit in small animal models, and the general concept of hydrogel introduction into the infarcted LV wall is undergoing clinical evaluation with the use of endovascular delivery approaches [18, 19] Codelivery of cells, growth factors, gene vectors, or drugs could also be options. The biomaterial coupled with a robotic delivery system described here represents an attractive technique that takes advantage of the phase change behavior of a bulking agent and robotic control systems to potentially achieve a planned intervention for patients at risk for cardiac failure after MI.

Supplementary Material

Refer to Web version on PubMed Central for supplementary material.

Acknowledgments

This work was financially supported by the US National Institutes of Health (grant R01 HL105911 and R01 HL078839). The authors wish to thank David Fischer and Judith Thoma for their expert help with surgical procedures in the porcine model.

References

1. Sutton MGSJ, Sharpe N. Left ventricular remodeling after myocardial infarction: pathophysiology and therapy. Circulation. 2000; 101:2981–8. [PubMed: 10869273]
2. Nelson DM, Ma Z, Fujimoto KL, Hashizume R, Wagner WR. Intra-myocardial biomaterial injection therapy in the treatment of heart failure: materials, outcomes and challenges. Acta Biomater. 2011; 7:1–15. [PubMed: 20619368]
3. Tous E, Purcell B, Ifkovits JL, Burdick JA. Injectable acellular hydrogels for cardiac repair. J Cardiovasc Transl Res. 2011; 4:528–42. [PubMed: 21710332]
4. Rane AA, Christman KL. Biomaterials for the treatment of myocardial infarction: a 5-year update. J Am Coll Cardiol. 2011; 58:2615–9. [PubMed: 22152947]
5. Ifkovits JL, Tous E, Minakawa M, et al. Injectable hydrogel properties influence infarct expansion and extent of postinfarction left ventricular remodeling in an ovine model. Proc Natl Acad Sci USA. 2010; 107:11507–12. [PubMed: 20534527]
6. 2012 Safety and feasibility of the injectable BL-1040 implant. Available at https://www.clinicaltrials.gov/ct2/show/NCT00 557531?term=Safety&and&Feasibility&of&the&Injectable&BL-1040&rank=1. Accessed April 15, 2015

Author Manuscript Author Manuscript Author Manuscript Author Manuscript

7. 2015 A study of VentriGel in early and late post-myocardial infarction patients. Available at https://www.clinicaltrials. gov/ct2/show/NCT02305602?term=ventrix&rank=1. Accessed April 15, 2015
8. 2012 Safety and feasibility of Algisyl-LVR™ as a method of left ventricular restoration in patients with DCM undergoing open-heart surgery. https://www.clinicaltrials.gov/ct2/show/ NCT00847964?term=Algisyl-LVR&rank=2. Accessed April 15, 2015
9. Seif-Naraghi SB, Singelyn JM, Salvatore MA, et al. Safety and efficacy of an injectable extracellular matrix hydrogel for treating myocardial infarction. Sci Transl Med. 2013; 5:173ra25.
10. Leor J, Tuvia S, Guetta V, et al. Intracoronary injection of in situ forming alginate hydrogel reverses left ventricular remodeling after myocardial infarction in swine. J Am Coll Cardiol. 2009; 54:1014–23. [PubMed: 19729119]
11. Ota T, Patronik NA, Schwartzman D, Riviere CN, Zenati MA. Minimally invasive epicardial injections using a novel semiautonomous robotic device. Circulation. 2008; 118:S115–20. [PubMed: 18824742]
12. Zhu Y, Jiang H, Ye SH, Yoshizumi T, Wagner WR. Tailoring the degradation rates of thermally responsive hydrogels designed for soft tissue injection by varying the autocatalytic potential. Biomaterials. 2015; 53:484–93. [PubMed: 25890745]
13. Patronik NA, Ota T, Zenati MA, Riviere CN. A miniature mobile robot for navigation and positioning on the beating heart. IEEE Trans Robot. 2009; 25:1109–24. [PubMed: 20179783]
14. Hartshorne, H.; Reynolds, JR. A System of Medicine. H.C. Lea's Son & Co; Philadelphia: 1880.
15. Wenk JF, Wall ST, Peterson RC, Helgerson SL, et al. A method for automatically optimizing medical devices for treating heart failure: designing polymeric injection patterns. J Biomech Eng. 2009; 131:121011. [PubMed: 20524734]
16. Fomovsky GM, Macadangdang JR, Ailawadi G, Holmes JW. Model-based design of mechanical therapies for myocardial infarction. J Cardiovasc Transl Res. 2011; 4:82–91. [PubMed: 21088945]
17. Patronik, NA. A miniature mobile robot for precise and stable access to the beating heart. Carnegie Mellon University; 2008. (Doctoral dissertation)
18. Fujimoto KL, Ma Z, Nelson DM, et al. Synthesis, characterization and therapeutic efficacy of a biodegradable, thermoresponsive hydrogel designed for application in chronic infarcted myocardium. Biomaterials. 2009; 30:4357–68. [PubMed: 19487021]
19. Nelson DM, Hashizume R, Yoshizumi T, Blakney AK, Ma Z, Wagner WR. Intramyocardial injection of a synthetic hydrogel with delivery of bFGF and IGF1 in a rat model of ischemic cardiomyopathy. Biomacromolecules. 2014; 15:1–11. [PubMed: 24345287]

Author Manuscript Author Manuscript Author Manuscript Author Manuscript

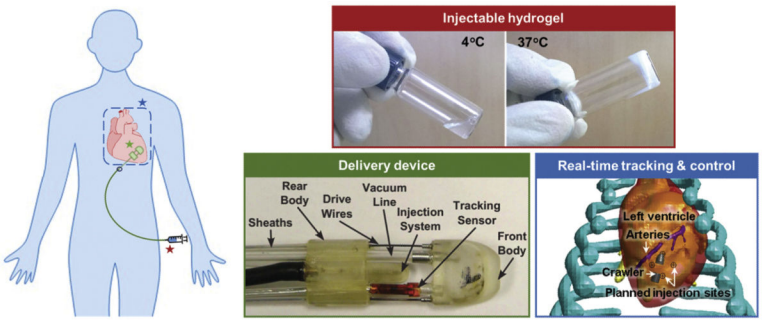

Fig 1.

Subxiphoid transepicardial injection of thermoresponsive hydrogel for myocardial injection therapy.

Author Manuscript Author Manuscript Author Manuscript Author Manuscript

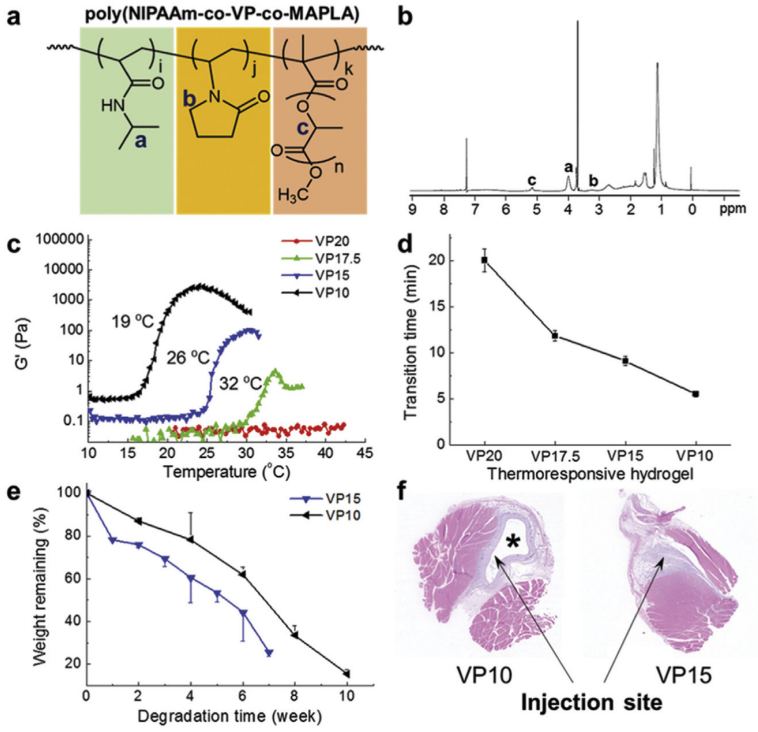

Fig 2.

(a) Composition of poly(NIPAAm-co-VP-co-MAPLA). (b) ^{1}H nuclear magnetic resonance (NMR) spectrum of poly(NIPAAm-co-VP-co-MAPLA) with feed ratio of 80:10:10 (VP10). (c) Shear modulus of poly(NIPAAm-co-VP-co-MAPLA) hydrogels under temperature change. (d) Transition time of poly(NIPAAm-co-VP-co-MAPLA) hydrogels in air. (e) Weight loss of VP10 and VP15 hydrogels in PBS. (f) Hematoxylin and eosin staining of rat hindlimb muscle 28 days after hydrogel injection: left, VP10; right, VP15. *Indicates the hydrogel mass. (NIPAAm = N-isopropylacrylamide; VP = N-vinylpyrrolidone; MAPLA = methacrylate-polylactide; PBS = phosphate buffer solution.)

Author Manuscript Author Manuscript Author Manuscript Author Manuscript

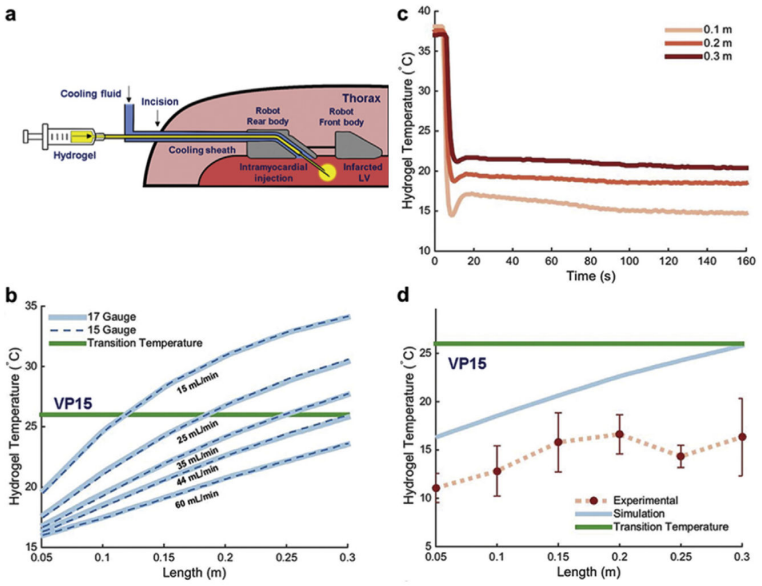

Fig 3.

(a) Components of the injection device (modified HeartLander) and illustration of transepicardial hydrogel injection with cooling. (b) Simulation of hydrogel temperature cooled by cooling fluids with different flow rates. (c) Simulated temporal change of 37°C hydrogel temperature at different positions in the catheter under cooling. (d) Measured hydrogel temperature along the cooled catheter, comparing with the simulated values and trasition temperature of VP15. (LV = left ventricle.)

Author Manuscript Author Manuscript Author Manuscript Author Manuscript

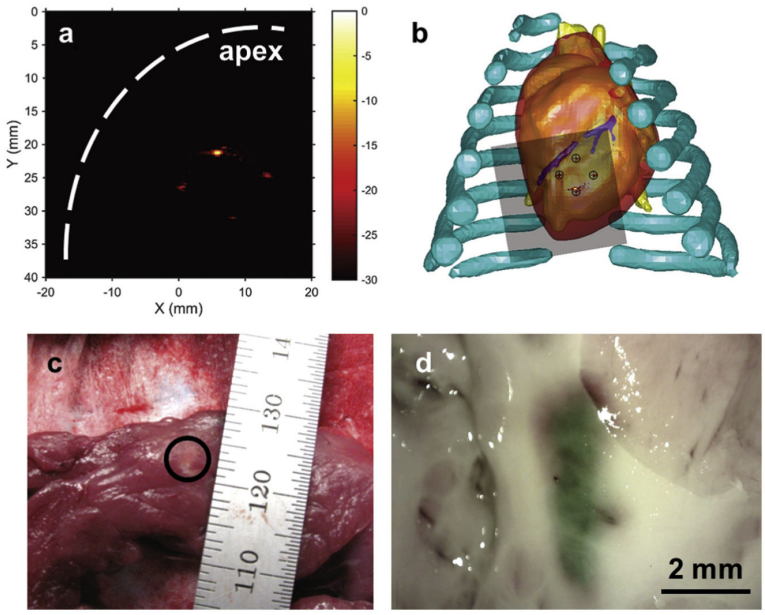

Fig 4.

(a) Photoacoustic imaging of patterned injections in a beating porcine heart, probing from the apex. The signals of injection sites away from apex were weaker because of energy loss through tissue. (b) Match between imaged injection sites with planned sites. (c) Injected hydrogel in the myocardium. (d) Deep injection of hydrogel on the endocardial side.